

Pharmacophore modeling of human adenosine receptor A_{2A} antagonists

Zhejun Xu · Feixiong Cheng · Chenxiao Da ·
Guixia Liu · Yun Tang

Received: 3 November 2009 / Accepted: 10 February 2010 / Published online: 12 March 2010
© Springer-Verlag 2010

Abstract Three-dimensional pharmacophore models of human adenosine receptor A_{2A} antagonists were developed based on 23 diverse compounds selected from a large number of A_{2A} antagonists. The best pharmacophore model, Hypo1, contained five features: one hydrogen bond donor, three hydrophobic points and one ring aromatic. Its correlation coefficient, root mean square deviation, and cost difference values were 0.955, 0.921 and 84.4, respectively, suggested that the Hypo1 model was reasonable and reliable. This model was validated by three methods: a test set of 106 diverse compounds, a simulated virtual screening, and superimposition with the crystal structure of A_{2A} receptor. The results showed that Hypo1 was not only in agreement with the A_{2A} crystal structure and literature reports, but also well identified active A_{2A} antagonists from the virtual database. This methodology provides helpful information and a robust tool for the discovery of potent A_{2A} antagonists.

Keywords Pharmacophore modeling · Adenosine receptor · A_{2A} antagonist · A_{2A} crystal structure · G-protein coupled receptor

Introduction

Adenosine is an endogenous purine nucleoside present in all tissues of mammalian organisms and that moderates a wide variety of functions and physiological effects, such as general depression of the central nervous system (striatum, nucleus accumbens and olfactory tubercles) and inhibition of platelet aggregation [1, 2]. Four distinct adenosine receptor subtypes have been identified to date, namely A_1 , A_{2A} , A_{2B} , and A_3 , all of which belong to the rhodopsin subfamily of G-protein coupled receptors (GPCRs) [3–5].

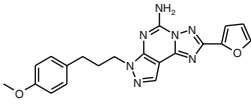
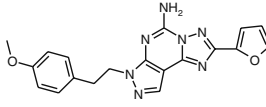
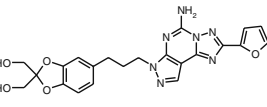
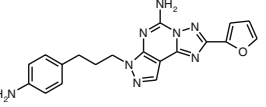
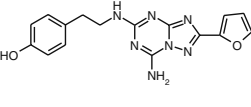
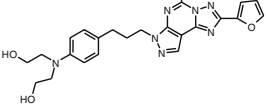
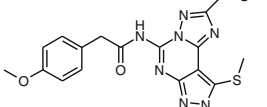
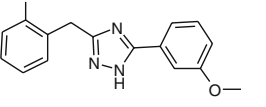
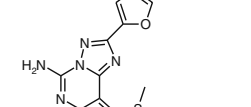
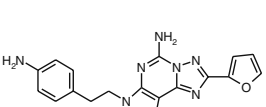
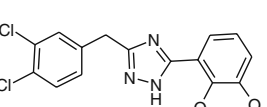
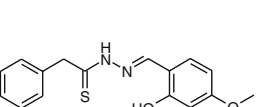
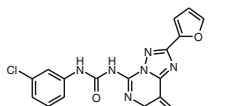
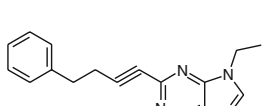
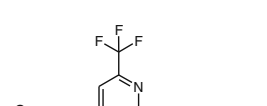
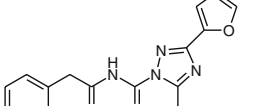
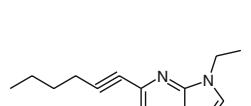
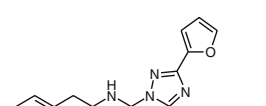
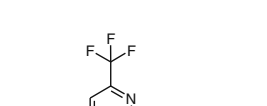
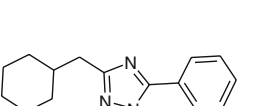
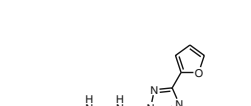
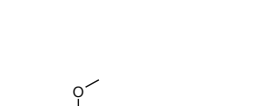
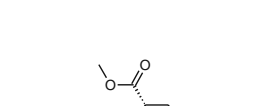
Among the four subtypes, the A_{2A} receptor is expressed particularly in the striatum, and distributed to a lower level in nucleus accumbens and olfactory tubercles in the rat and human brain [6]. It can form functional heteromeric complexes with other GPCRs, such as dopamine D_2 , metabotropic glutamate mGlu5, and adenosine A_1 receptors [7, 8]. Available evidence suggests that selective A_{2A} antagonists have potential as novel therapeutic agents for the treatment of neurodegeneration, including Parkinson's disease [9–12].

Over the past decade, a large number of selective, orally available A_{2A} antagonists have been reported as agents for the treatment of Parkinson's disease. They can be divided into four types, namely adenine derivatives, adenine analogs, xanthine and non-xanthine derivatives [13–23]. As shown in Table 1, compound **1** (SCH442416) has high selectivity for the A_{2A} receptor versus the other adenosine receptor subtypes. It also possesses excellent pharmacokinetics properties, such as more favorable blood–brain barrier (BBB) permeability potential. Also, the in vivo metabolism of compound **1** is very slow [13]. Compound **5** (ZM241385) also has about 50-fold selectivity for A_{2A} receptor versus A_{2B} receptor [16]. With the trend for increasing incidence of neurodegenerative diseases (e.g.,

Electronic supplementary material The online version of this article (doi:10.1007/s00894-010-0690-z) contains supplementary material, which is available to authorized users.

Z. Xu · F. Cheng · C. Da · G. Liu · Y. Tang (✉)
School of Pharmacy,
East China University of Science and Technology,
130 Meilong Road,
Shanghai 200237, China
e-mail: ytang234@ecust.edu.cn

Table 1 Chemical structures of A_{2A} antagonists in training set with binding affinity (K_i , nM) for HypoGen run

			
1 ($K_i=0.048$ nM) [13]	2 ($K_i=0.19$ nM) [14]	3 ($K_i=0.22$ nM) [15]	4 ($K_i=0.8$ nM) [14]
			
5 ($K_i=1.1$ nM) [16]	6 ($K_i=15$ nM) [17]	7 ($K_i=20$ nM) [18]	8 ($K_i=22$ nM) [15]
			
9 ($K_i=55$ nM) [14]	10 ($K_i=90$ nM) [18]	11 ($K_i=100$ nM) [18]	12 ($K_i=100$ nM) [18]
			
13 ($K_i=150$ nM) [19]	14 ($K_i=290$ nM) [20]	15 ($K_i=310$ nM) [15]	16 ($K_i=390$ nM) [21]
			
17 ($K_i=400$ nM) [15]	18 ($K_i=450$ nM) [20]	19 ($K_i=700$ nM) [18]	20 ($K_i=2000$ nM) [22]
			
21 ($K_i=4200$ nM) [18]	22 ($K_i=6900$ nM) [18]	23 ($K_i=19000$ nM) [22]	

Parkinson's disease), the need development of A_{2A} antagonists with excellent pharmacokinetic properties and high selectivity is becoming very urgent.

Recently, the three-dimensional (3D) structure of the A_{2A} receptor complexed with antagonist **5** was determined by X-ray crystallography, which provided detailed information on the interaction between the receptor and antagonist [24]. However, it was only a static map and could not account for all reported A_{2A} antagonists. Structure-based techniques generally could not accurately predict binding affinity due to the limitation of scoring functions and the flexibility of the biomacromolecule. In order to enhance our understanding of the antagonistic mechanism, and to facilitate the discovery of new A_{2A} antagonists, other methods, such as pharmacophore modeling, are needed.

A pharmacophore model describes the spatial arrangement of essential structural features common to a set of active compounds. This concept has proven extremely successful, not only in rationalizing structure–activity relationships, but also in developing the appropriate 3D-tools for efficient virtual screening [25, 26]. Pharmacophore modeling has been widely used in drug discovery. In a recent study on A_{2A} antagonists, Mantri et al. [27] developed a pharmacophore model by overlapping the nonxanthine type of known A_{2A} antagonists, and then synthesized a new class of compounds with 2-amininicotinonitrile that showed high affinity towards the human A_{2A} adenosine receptor. This model was based on a series of non-xanthine compounds, thus it had limited applicability for other A_{2A} antagonists. Another 3D pharmacophore model for A_{2A} antagonists was generated by Wei et al. [28] using the HipHop module within the CATALYST software. But the training set for this model had no structure diversity since all compounds were derived from the same skeleton, which had a furan ring and a 2-amino nicotinonitrile moiety. It is clear that the development of a pharmacophore with diverse A_{2A} antagonists is required with high priority.

In the present study, a pharmacophore model was developed from a diverse set of A_{2A} antagonists, including compound **5** in the A_{2A} crystal structure, using CATALYST software [29]. The proposed model was validated using a wide, structurally diverse, test set; an enrichment factor; specific comparison with the binding model of the A_{2A} receptor crystal structure; and reported pharmacophore models.

Materials and methods

All modelling in this study was carried out on a PC cluster running Redhat Linux WS 4.0. Pharmacophore models were generated by CATALYST 4.11 [29] implemented in Discovery Studio 2.1.

Dataset preparation

A total of 129 different human A_{2A} antagonists included the following chemical classes: pyrazolotriazolopyrimidine derivatives, 9-ethyladenine derivatives, trifluoropyrimidine derivatives, thioacyhydrazone derivatives and 1,2,4-triazole derivatives collected from the published literature [13–23]. Achiral antagonists and one antagonist with known absolute configuration (**23** in Table 1) were employed for modeling. Among this set, 23 diverse compounds whose binding affinities (K_i values) ranged from 0.048 nM to 19,000 nM (over six orders of magnitude) were selected as the training set (Table 1) and the others served as a test set (see electronic supplementary material, Table S1). In general, CATALYST requires a training set containing at least 16 compounds whose bioactivities are evenly spread over at least four orders of magnitude [29].

Pharmacophore modeling

All compounds were drawn with CATALYST 2D/3D sketcher, and energy minimized using the CHARMM-like force field incorporated in the software. Conformers of all compounds were then generated using the 'best quality' option within the CATALYST Conform module. The maximum number of conformers was set at 250 and the energy range was set to 20.0 kcal mol⁻¹ above the global energy minimum. All conformers were used in subsequent pharmacophore generation.

The HypoGen module implemented in CATALYST 4.11 was used to create the pharmacophore models, and default settings were used except where specified in Table 2. Five pharmacophore features were selected from the feature dictionary of CATALYST based on previous A_{2A} pharma-

Table 2 Selected input features and Catalyst running parameters employed in pharmacophore model run. *HBA* Hydrogen-bond acceptor, *HBD* hydrogen-bond donor, *RA* ring aromatic, *HY* hydrophobic, *PI* positively ionizable

Run no.	Selected input features: type and range					
	HBA	HBD	HY	RA	PosIon	Max–min
1	0–5	0–5	0–5	0–5	0–5	4–7
2	0–5	0–5	0–5	0–5	1–5	5–8
3	0–5	1–5	1–5	0–5	1–5	4–7
4	0–5	0–5	0–5	1–5	0–5	5–8
5	1–5	0–5	0–5	1–5	0–5	5–8
6	0–5	0–5	0–5	1–5	1–5	4–7
7	1–5	1–5	0–5	1–5	0–5	5–8
8	1–5	0–5	0–5	0–5	1–5	5–8
9	0–5	1–5	0–5	0–5	05	5–8
10	0–5	1–5	1–5	1–5	0–5	5–8

cophore studies and A_{2A} antagonist chemical features, namely hydrogen-bond acceptor (HBA), hydrogen-bond donor (HBD), ring aromatic (RA), hydrophobic (HY), and positively ionizable (PI). The uncertainty value was set as 3.0. Ten pharmacophore models with top ranking cost function were generated and saved for further analysis.

The quality of the HypoGen model is well described in the CATALYST user guide [29], including fixed cost, null cost, total cost, and other statistical parameters. The total cost of the generated pharmacophores can be calculated from the deviation between the estimated activity and the observed activity, combined with the complexity of the hypothesis (the number of pharmacophore features). A null cost can be calculated based on the assumption that there is no relationship in the data, and that the experimental activities are normally distributed about their mean. Hence, the greater the difference between the null cost of the generated hypothesis and the total cost, the more likely it is that the hypothesis does not reflect a chance correlation.

Validation of pharmacophore model

The pharmacophore models selected by cluster and cost analysis were then validated in two subsequent steps: test set prediction, and enrichment factor of simulated virtual screening database. A set of 106 diverse A_{2A} antagonists were used to identify the best model that could accurately evaluate the binding affinity of A_{2A} antagonists based on Fischer's randomization test on 95% confidence level [29, 30]. Then, the total simulated virtual screening database, containing 2,000 molecules selected randomly from Specs compounds database, and another 115 molecules selected from literature reports, were subjected to the enrichment factor test. The 115 molecules included 25 known active A_{2A} antagonists, 10 known active A_{2A} agonists, 10 A_{2B} antagonists, 10 A_{2B} agonists, 10 A_1 antagonists, 10 A_1 agonists, 10 A_3 antagonists, 10 A_3 agonists, 10 delta-opioid antagonists and 10 delta-opioid agonists (Tables 3, S2). The enrichment factor (E) was calculated according to Eq. 1.

$$E = Ha/Ht \div A/D \quad (1)$$

where Ht represents the number of hits retrieved, Ha represents the number of active molecules in the hit list, A represents the number of active molecules present in the database, and D is the total number of molecules in database [31].

Mapping of pharmacophore model onto the A_{2A} crystal structure

A recent paper provided the high-resolution crystal structure of the A_{2A} receptor complexed with antagonist **5**. The best pharmacophore model aligned with compound **5** was superimposed into the active site by the pharmacophore protocol

implemented in Discovery Studio 2.1 [32]. The pharmacophore feature and key residues were then analyzed.

Results and discussion

Construction of pharmacophore model

The pharmacophore models were developed on the basis of 23 diverse compounds in the training set (Table 1). A test set of another 106 compounds (activities spanning from 0.12 nM to 8,100 nM, Table S1) and a simulated virtual screening database of 2,115 molecules (Table S2 and Table 3) were used to validate the model.

Initially, ten trials were carried out with the HBA, RA, HY, HBD, and/or PI features to explore the CATALYST running parameters (Table 2). The results are listed in Table 4. The RMSD values, correlation coefficients and other cost criteria in Table 4 were compared to evaluate the quality of the ten trials. Trials 2, 6 and 9 were found better than the others, but the configuration values of Trials 2 and 6 were greater than 17 (Table 4). In general, the configuration value should be lower than 17 according to the user guide of CATALYST [29]. Hence, Trial 9 was regarded as the best, and was selected for further validation.

The ten hypotheses with top ranking scores were then generated for Trial 9. As shown in Table 5, the null cost of the ten hypotheses was 187, the fixed cost and the configuration value were 92.2 and 13.7 (<17), respectively. The Δ cost (null cost – total cost) range from 74.7 to 84.4 was an indication of more than 90% predictive reliability coefficient. For a meaningful pharmacophore hypothesis, the total cost should be close to the fixed cost, and there must be a large difference between null and total cost. A value of 40–60 bits of Δ cost indicated that the model had a predictive reliability coefficient between the experimental and predicted activities of 75–90%. All ten hypotheses showed high training correlation coefficients ($R_{\text{tr-set}}$) between experimental and predicted K_i values, in the range of 0.904–0.955.

From Table 5, cluster analysis showed that the entire ten hypotheses had the same pharmacophore feature, including one HBD, three HYS and one RA. Among them, Hypo1 had the best cost values and other statistical parameters, thus Hypo1 was selected as the best pharmacophore model. The 3D spatial arrangement and distance constraints of all features in Hypo1 are illustrated in Fig. 1a,b.

Values for experimental activity, predicted activity, fit value, error cost and predicted active scale of Hypo1 to the training set are listed in Table 6. Most of the predicted K_i values were found to be of the same order of magnitude as experimental values. In the training set, all highly active compounds mapped to all features of the pharmacophore model. And almost all moderately active molecules in the

Table 3 Statistical results for simulated virtual screening database

No.	Parameter	Number of compounds
1	Total molecules in database (D)	2,115
2	Total number of active molecules in database (A)	25
3	Total hits (Ht)	190
4	Active hits (Ha)	25
5	Enrichment factor (E)	11.1
6	Number of A ₁ antagonists in database (hits)	10 (2)
7	Number of A ₁ agonists in database (hits)	10 (0)
8	Number of A _{2A} agonists in database (hits)	10 (0)
9	Number of A _{2B} antagonists in database (hits)	10 (5)
10	Number of A _{2B} agonists in database (hits)	10 (0)
11	Number of A ₃ antagonists in database (hits)	10 (0)
12	Number of A ₃ agonists in database (hits)	10 (0)
13	Number of delta-Opioid antagonists in database (hits)	10 (0)
14	Number of delta-Opioid agonists in database (hits)	10 (0)

training set were mapped onto the HY2 and HBD, revealing that these two features were essential for molecular bioactivity and thus should be taken into account when designing the novel A_{2A} antagonists.

The fitness of the most active compound was 11.1 when mapped onto the Hypo1, whereas the least active compound **23** had a fitness of only 5.30. Compound **1** was mapped onto all features of Hypo1, while compound **23** lacked the HBD feature and the HY1 feature (Fig. 1c,d). This showed that our model could well predict high and low binding affinity of A_{2A} antagonists. In compound **1**, the HBD feature corresponded to a conserved amino group, RA mapped to the planar aromatic core of the bicyclic triazolotriazine core, and the

furan ring, aliphatic hydrocarbon and benzene ring mapped to the hydrophobic (HY) features, respectively (Fig. 1c).

Validation of pharmacophore model

The predictive ability of the best score hypothesis (Hypo1) was first validated with a test set of 106 diverse A_{2A} antagonists, which were grouped into highly active (≤ 10 nM, +++), moderately active (10–5,000 nM, ++), and low active ($\geq 5,000$ nM, +). A test set correlation coefficient ($R_{\text{test-set}}$) of 0.805 showed good correlation between experimental and predicted activities. A plot showing the correlation between experimental and predicted activities for test set and training

Table 4 General performance of pharmacophore models generated for A_{2A} antagonists. *R* Correlation coefficient, *RMSD* root mean squares deviation

Running No.	Cost criteria					
Trial	R range	RMSD range	Configuration	Total cost range ^a	Fixed cost	Δ Cost range ^b
1	0.90–0.95	1.04–1.36	18.31	133–143	117	42.6–53.7
2	0.88–0.93	1.14–1.44	16.20	110–118	94.7	68.3–76.8
3	0.84–0.87	1.54–1.66	12.09	118–123	90.6	63.4–68.8
4	0.85–0.95	0.94–1.38	13.84	106–118	96.3	68.5–80.3
5	0.87–0.90	1.32–1.52	16.47	116–123	95.0	63.5–70.4
6	0.90–0.95	1.00–1.30	17.38	108–118	95.9	69.0–79.2
7	0.86–0.89	1.38–1.58	14.67	118–122	93.2	64.5–69.0
8	0.87–0.93	0.93–1.15	15.41	110–122	93.9	64.8–76.9
9	0.90–0.95	0.92–1.32	13.70	102–112	92.2	74.7–84.4
10	0.90–0.93	1.11–1.35	15.48	140–149	120.9	37.4–46.9

^a Total cost of the generated pharmacophore models calculated from the deviation between predicted activity and experimental activity, combined with the complexity of the hypothesis (i.e., number of pharmacophore features)

^b Δ Cost = null costs–total costs; null cost value was 187 bits. A null cost that presumes no relationship in the data, and that the experimental activities are distributed normally about their mean can also be calculated. All criteria values were reported in log files of each automatic HypoGen run and all cost units are given in bits

Table 5 Statistical parameters of the top hypotheses for the A_{2A} pharmacophore model generated

Hypo no.	Total cost ^a	ΔCost ^b	RMSD	R _{tr-set} correlation	R _{test-set} correlation
1	102	84.4	0.921	0.955	0.805
2	104	83.2	0.978	0.948	0.791
3	108	79.2	1.16	0.927	0.774
4	108	79.1	1.15	0.927	0.768
5	110	77.0	1.24	0.916	0.749
6	110	76.3	1.26	0.913	0.737
7	111	76.1	1.27	0.912	0.731
8	111	75.9	1.27	0.911	0.713
9	112	75.2	1.27	0.911	0.708
10	112	74.7	1.32	0.904	0.698

^a Total cost of generated pharmacophore models calculated from the deviation between predicted and experimental activity, combined with the complexity of the hypothesis (i.e., number of pharmacophore features)

^b ΔCost=(null cost–total cost); null cost value was 186, fixed cost value was 92.2, configuration cost value is 13.7, all cost units are given in bits. Ten hypothesis have the same five features: 1 HBD, 1 RA, 3 HY

set molecules is presented in Fig. 2. The RMSE (root mean square error) was only 0.559 for the test set, which was lower than the RMSD of the training set (0.921). This indicated that the pharmacophore model was able to predict the activity of unknown molecules with reasonable accuracy. In more detail, 11 of 17 highly active antagonists, 88 of 88 moderately active antagonists, and 1 of 1 inactive antagonists were correctly predicted, and only 6 highly active compounds were underestimated as moderately active compounds. The most active compound in the test set had a fitness score of 10.8 (compound **3** in Table S1) when it was mapped onto Hypo1 and all features were correctly mapped. In summary, most compounds in the test set could be well predicted.

Hypo1 was then evaluated for the ability to detect active A_{2A} antagonists from the simulated virtual screening database described in the Materials and methods section.

The results demonstrated that 190 molecules, including all 25 known active A_{2A} antagonists, were retrieved as hits. Though 2 A₁ antagonists and 5 A_{2B} antagonists were also picked out, A₃ antagonists, delta-opioid antagonists and all agonists were not included (Table 3). Thus, the enrichment factor (Eq. 1) was calculated to be 11.1, which indicated an 11 times greater probability of detecting active compounds from the virtual database than an inactive one. However, there was some limit to the ability to accurately distinguish different adenosine subtypes.

Ligand and crystal structure-based consensus predictive model

Recently, the crystal structure of the A_{2A} receptor with antagonist **5** was determined by Jaakola et al. [24]. It was used to further evaluate the best hypothesis (Hypo1). The

Fig. 1a–d The best hypothesis model Hypo1 of A_{2A} antagonists generated by the HypoGen module in CATALYST 4.11. **a** Best pharmacophore model Hypo1. **b** Three-dimensional (3D) spatial arrangement and geometric parameters of pharmacophore features (Å). **c** Hypo1 aligned with the most active compound **1** ($K_i = 0.048$ nM). **d** Hypo1 mapped with the low active compound **23** ($K_i = 19,000$ nM). Color-coding of pharmacophore features: *magenta* Hydrogen-bond donor (HBD), *cyan* hydrophobic (HY), *orange* ring aromatic (RA)

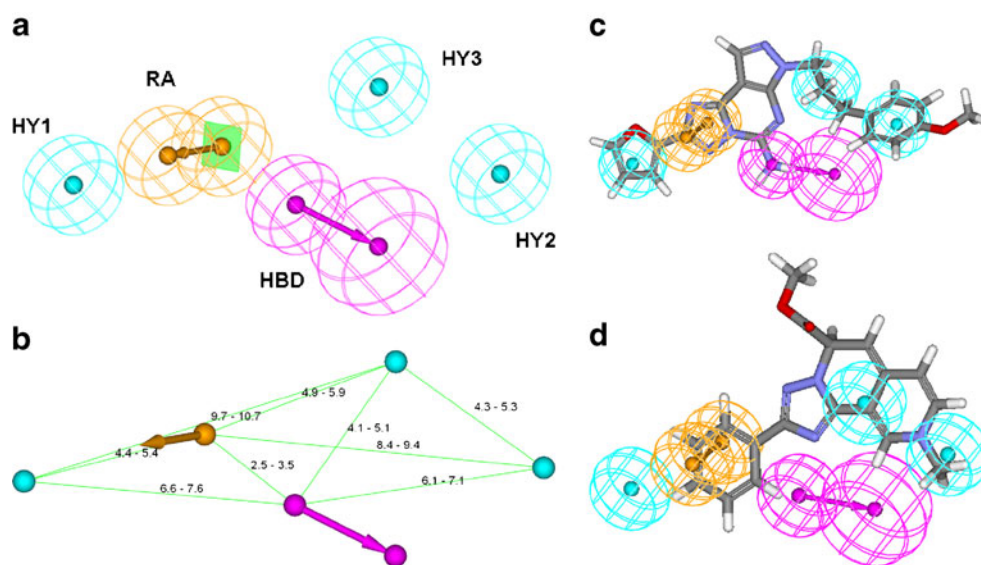


Table 6 Experimental and predicted (Hypo1) binding affinity (K_i , nM) for training set molecules

Compound no.	K_i (nM)		Fit value ^a	Error cost ^b	Activity scale ^c		Mapped features				
	Predicted	Experimental			Estimated	Actual	HBD	HY1	HY2	HY3	RA
1	0.038	0.048	11.1	-1.3	+++	+++	+	+	+	+	+
2	0.21	0.19	10.4	1.1	+++	+++	+	+	+	+	+
3	0.28	0.22	10.3	1.3	+++	+++	+	+	+	+	+
4	12	0.8	8.61	16	++	+++	+	+	+	+	+
5	1	1.1	9.70	-1.1	+++	+++	+	+	+	+	+
6	14	15	8.55	-1	++	++	-	+	+	+	+
7	62	20	7.92	3.1	++	++	+	+	+	+	-
8	15	22	8.53	-1.4	++	++	+	-	+	+	+
9	20	55	8.40	-2.7	++	++	+	-	+	+	+
10	39	90	8.12	-2.3	++	++	+	+	+	+	+
11	460	100	7.05	4.6	++	++	+	+	+	+	-
12	100	100	7.70	-1	++	++	-	+	+	+	+
13	190	150	7.44	1.2	++	++	+	-	+	+	+
14	270	290	7.27	-1.1	++	++	-	+	+	+	+
15	960	310	6.73	3.1	++	++	-	+	+	-	+
16	270	390	7.28	-1.5	++	++	+	-	+	+	+
17	240	400	7.32	-1.6	++	++	-	+	+	+	+
18	1,500	450	6.52	3.4	++	++	-	+	+	-	+
19	270	700	7.28	-2.6	++	++	+	+	+	+	-
20	730	2,000	6.85	-2.8	++	++	-	+	+	+	+
21	1,200	4,200	6.64	-3.6	++	++	-	+	+	+	-
22	1,100	6,900	6.69	-6.5	++	+	-	-	+	+	+
23	26,000	19,000	5.30	1.4	+	+	-	+	-	+	+

^a Fit value indicates how well the features in the pharmacophore overlap the chemical features in the molecule. Fit = weight \times [max(0.1 - SSE)] where SSE = (D/T)², D = displacement of the feature from the center of the location constraint and T = the radius of the location constraint sphere for the feature

^b + Predicted K_i is higher than experimental K_i ; - predicted K_i is lower than experimental K_i ; 1 predicted K_i is equal to experimental K_i

^c +++ Highly active ($K_i \leq 10$ nM), ++ moderately active ($K_i = 10$ –5,000 nM), + low active ($K_i \geq 5,000$ nM)

binding cavity is composed of residues Ala63, Ile66, Ala81, Val84, Leu85, Phe168, Glu169, Met174, Met177, Trp246, Leu249, Asn253, Ile274, Ser277, and His278. Compound **5** from the crystal structure was fitted well with all features of Hypo1. As shown in Fig. 3a, the HBD mapped to the conserved amino group, and the RA group mapped to the planar aromatic core of the bicyclic triazolotriazine core. The furan ring, aliphatic hydrocarbon and benzene ring mapped to the three HY features, respectively. When superimposing the best mapping conformation (gray in Fig. 3b) of the pharmacophore model with the crystal binding conformation of compound **5** (blue), they fitted well to each other (Fig. 3b). This indicated that Hypo1 could map all the essential features of the A_{2A} crystal structure.

Figure 3c presents the superimposition of Hypo1 with the active site of the human A_{2A} receptor. Clearly, the HBD of Hypo1 corresponds to the hydrogen-bond interaction between the carboxyl motif of Glu169, and the length of

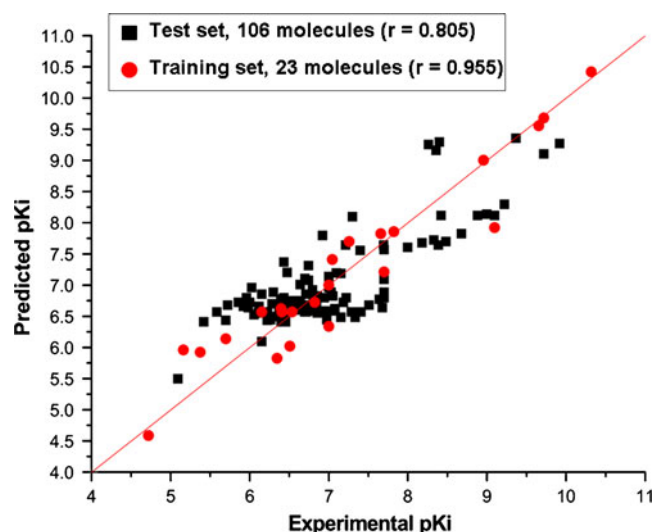


Fig. 2 Graph showing the correlation (r) between experimental and predicted activities [$pK_i = -\log(K_i \times 10^{-9})$] for the 106 test set and 23 training set molecules against Hypo1 model for A_{2A} antagonists

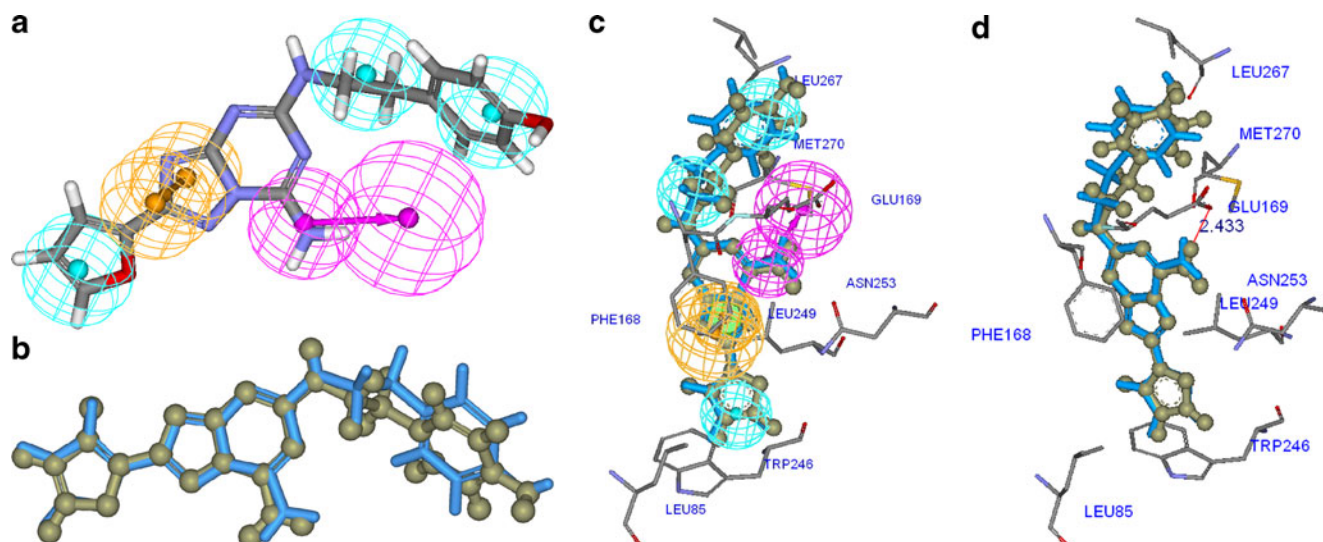


Fig. 3a–d Comparing the conformation generated by pharmacophore mapping with conformation of the crystal complex for compound **5** (PDB code: 3EML). **a** Hypo1 aligned with compound **5**. **b** Pharmacophore mapping conformation (gray) of Hypo1 superimposed on the crystal conformation of compound **5** (blue). **c** Hypo1 mapped onto compound

5 superimposed on the active site of the A_{2A} crystal structure. **d** Hydrogen-bond distances between the ligand NH_2 and the Glu169 carboxylate. Color-coding of pharmacophore features: magenta HBD, cyan HY, orange RA

this hydrogen-bond is only 2.43 Å (Fig. 3d). In the A_{2A} receptor, mutation of Glu169 to alanine reduced the binding affinity for both antagonists and agonists [33]. And the phenyl group of Phe168 formed a π - π stacking interaction with the purine scaffold of compound **5**. The phenyl ring substitution in the region surrounded by Leu267 and Met270 discriminated HY as more suitable than RA. The furan ring motif within the ligand was deep in the active site surrounded by residues Leu85, Trp246, Leu249 to form hydrophobic interactions.

Comparison with previously reported models

In 2007, a 3D pharmacophore model for A_{2A} antagonists was generated by Wei et al. [28] using the HipHop module of CATALYST program. This model consisted of four features: one RA feature, one PI feature, one HBA lipid feature, and one HY feature. Comparing with model Hypo1 in this paper, some differences between the two models are evident. First, the amino group displayed as positively ionizable, while it was recognized as HBD in Hypo 1, which is consistent with analysis of the crystal structure. Another difference was part of the furan ring of compound **5**, which was defined as an HY feature in Hypo1; however, it was identified as HBA in the paper of Wei et al. [28]. In the A_{2A} crystal structure, the furan ring of compound **5** was located in the hydrophobic pocket of Trp246 and Leu85, so was more favorable for the HY feature (see Fig. 3c).

Recently a pharmacophore hypothesis was derived from nonxanthine type A_{2A} antagonists by Mantri et al. [27]. This model included four features: one HYD, one N-containing

RA and two lipophilic groups. These features were consistent with those in our Hypo1 model. Mapping analysis of our model also confirmed the hypothesis that hydrophobic areas (HY2, HY3) linked to an aromatic ring are key for binding to the receptor.

Comparing the two models, our model was superior in two aspects: diverse structures of compounds were used in

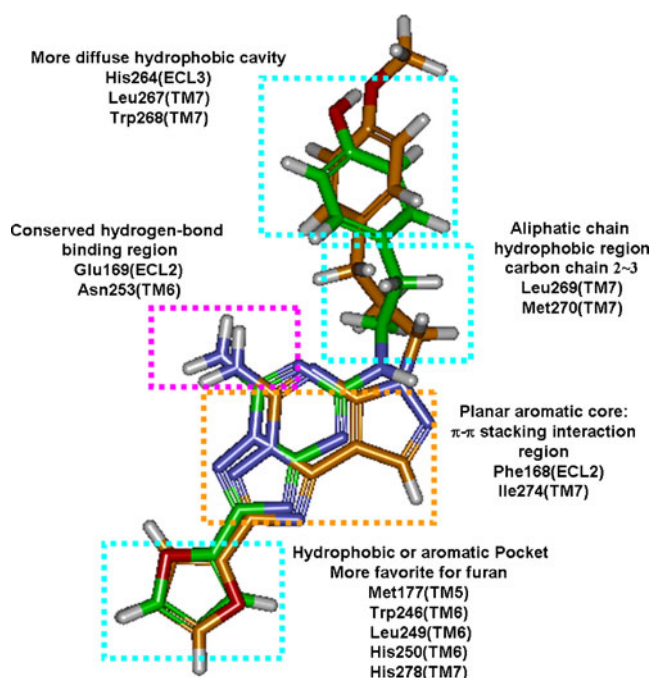


Fig. 4 Proposed modifications of A_{2A} antagonists based on the superimposition of pyrazolotriazolopyrimidine derivatives (Compound **1**, brown) with compound **5** (green) in crystal complex

our training set, and the $R_{\text{tr-set}}$, $R_{\text{test-set}}$ and other cost values were better; furthermore, Hypo1 was consistent with A_{2A} crystal structure and mutation data.

Implications for identification of novel A_{2A} antagonists

One of the key goals of computer-aided molecular design methods in modern medicinal chemistry is to discover or design new bio-active candidate compounds. The pharmacophore approach has proven successful in this field [34–36]. A good pharmacophore model not only helps us visualize the potential interaction between target and ligand, but also enriches screening experiments aimed at the discovery of novel bio-active compounds [36]. Thus, the construction of a robust pharmacophore is a key objective in many drug discovery efforts.

After generating an A_{2A} antagonist pharmacophore model, two approaches can be used to identify new A_{2A} antagonists. On the one hand, using virtual screening, the pharmacophore model can be used to search a database; hits are then refined by molecular docking based on the crystal structure of the receptor. On the other hand, molecular docking can be used to screen a database first, with hits then being refined by pharmacophore model. There are many good examples to demonstrate highly active lead compounds identified by pharmacophore searches or pharmacophore models combined with molecule docking methods [36, 37].

The superimposition of pyrazolotriazolopyrimidine derivative compound **1** with compound **5** in the A_{2A} crystal structure showed that a highly active A_{2A} antagonist should comprise five regions: a planar aromatic core, a conserved HBD binding region, a hydrophobic or aromatic pocket, an aliphatic chain hydrophobic region, and one more diffuse hydrophobic region (Fig. 4). In detail, the planar aromatic core should form π – π stacking with residues of Phe168 in the second extracellular loop. The exocyclic amine on the planar aromatic core provides a polar hydrogen, which forms one of the hydrogen-bond interactions with residue Glu169, so it may be important for activity. The hydrophobic or aromatic pocket was favorable for furan, but other compounds with other aromatic groups were also available. Lots of highly active A_{2A} antagonists had one aliphatic chain hydrophobic region that connected the diffuse hydrophobic cavity, and the length of the chain should be two or three carbons. In summary, these results provide helpful information and robust tools for the discovery of potent A_{2A} antagonists.

Conclusions

In the present work, 3D pharmacophore modeling was developed for A_{2A} antagonists based on a training set of 23 compounds using the HypoGen module of CATALYST

software. The best quantitative model (Hypo1) contained one HBD, three HY, and one RA, and the correlation coefficient of the training set was 0.955. Mapping of the most active and inactive molecules indicated that the HY2 and HBD groups played a key role in binding of A_{2A} antagonists to their receptor.

The correlation coefficient of Hypo1 based on 106 test set compounds was 0.805, which showed that this model could predict the binding affinity of A_{2A} antagonists over a wide range. The high enrichment factor value 11.1 of simulated virtual database screening for pharmacophore models indicated the good ability of the model to detect active compounds from a virtual database. This procedure could be widely used in virtual screening for developing novel A_{2A} antagonists.

The pharmacophore mapping conformation of antagonist **5** was compared with its conformation in the active site of the A_{2A} receptor in the crystal structure complex. The pharmacophore model could also correctly reflect the interactions between the A_{2A} receptor and antagonists. Hence, the pharmacophore model Hypo1 can be used as a 3D query in database searching to identify novel A_{2A} antagonists and to predict their binding affinities before undertaking further study.

Acknowledgments This work was supported by the Program for New Century Excellent Talents in University (No. NCET-08-0774), the 863 High-Tech Project (No. 2006AA020404) and the 111 Project of China (No. B07023). The authors greatly appreciated Dr. Philip W. Lee for his valuable suggestions in improving the quality of the manuscript.

References

- Poulsen SA, Quinn RJ (1998) Adenosine receptors: new opportunities for future drugs. *Bioorg Med Chem* 6:619–641
- Fredholm BB, Abbracchio MP, Burnstock G, Daly JW, Harden TK, Jacobson KA, Leff P, Williams M (1994) Nomenclature and classification of purinoceptors. *Pharmacol Rev* 46:143–156
- Fredholm BB, IJ AP, Jacobson KA, Klotz KN, Linden J (2001) International union of pharmacology. XXV. Nomenclature and classification of adenosine receptors. *Pharmacol Rev* 53:527–552
- Feoktistov I, Biaggioni I (1997) Adenosine A2B receptors. *Pharmacol Rev* 49:381–402
- Ralevic V, Burnstock G (1998) Receptors for purines and pyrimidines. *Pharmacol Rev* 50:413–492
- Moreau JL, Huber G (1999) Central adenosine A(2A) receptors: an overview. *Brain Res Brain Res Rev* 31:65–82
- Schwarzschild MA, Agnati L, Fuxe K, Chen JF, Morelli M (2006) Targeting adenosine A_{2A} receptors in Parkinson's disease. *Trends Neurosci* 49:647–654
- Johansson B, Georgiev V, Fredholm BB (1997) Distribution and postnatal ontogeny of adenosine A2A receptors in rat brain: comparison with dopamine receptors. *Neuroscience* 80:1187–1207
- Pinna A, Wardas J, Simola N, Morelli M (2005) New therapies for the treatment of Parkinson's disease: adenosine A2A receptor antagonists. *Life Sci* 77:3259–3267
- Gerkens JF (1974) Effect of long-term treatment with guanidine or guanethidine on sympathetic function. *Eur J Pharmacol* 26:143–150

11. Kim DS, Palmiter RD (2003) Adenosine receptor blockade reverses hypophagia and enhances locomotor activity of dopamine-deficient mice. *Proc Natl Acad Sci USA* 100:1346–1351
12. Ongini E, Fredholm BB (1996) Pharmacology of adenosine A2A receptors. *Trends Pharmacol Sci* 17:364–372
13. Todde S, Moresco RM, Simonelli P, Baraldi PG, Cacciari B, Spalluto G, Varani K, Monopoli A, Matarrese M, Carpinelli A, Magni F, Kienle MG, Fazio F (2000) Design, radiosynthesis, and biodistribution of a new potent and selective ligand for in vivo imaging of the adenosine A(2A) receptor system using positron emission tomography. *J Med Chem* 43:4359–4362
14. Baraldi PG, Cacciari B, Romagnoli R, Spalluto G, Monopoli A, Ongini E, Varani K, Borea PA (2002) 7-Substituted 5-amino-2-(2-furyl)pyrazolo[4, 3-e]-1, 2, 4-triazolo[1, 5-c]pyrimidines as A2A adenosine receptor antagonists: a study on the importance of modifications at the side chain on the activity and solubility. *J Med Chem* 45:115–126
15. TM BPG, Romagnoli R, Kashef HE, Preti D, Bovero A, Fruttarolo F, Gordaliza M, Borea PA (2006) Pyrazolo[4, 3-e][1, 2, 4]triazolo[1, 5-c]pyrimidine template: organic and medicinal chemistry approach. *Curr Org Chem* 10:259–275
16. Poucher SM, Keddie JR, Singh P, Stoggall SM, Caulkett PW, Jones G, Coll MG (1995) The in vitro pharmacology of ZM 241385, a potent, non-xanthine A2a selective adenosine receptor antagonist. *Br J Pharmacol* 115:1096–1102
17. Baraldi PG, Fruttarolo F, Tabrizi MA, Preti D, Romagnoli R, El-Kashef H, Moonman A, Varani K, Gessi S, Merighi S, Borea PA (2003) Design, synthesis, and biological evaluation of C9- and C2-substituted pyrazolo[4, 3-e]-1, 2, 4-triazolo[1, 5-c]pyrimidines as new A2A and A3 adenosine receptors antagonists. *J Med Chem* 46:1229–1241
18. Alanine A, Anselm L, Steward L, Thomi S, Vifian W, Groaning MD (2004) Synthesis and SAR evaluation of 1, 2, 4-triazoles as A (2A) receptor antagonists. *Bioorg Med Chem Lett* 14:817–821
19. Volpini R, Costanzi S, Lambertucci C, Vittori S, Martini C, Trincavelli ML, Klotz KN, Cristalli G (2005) 2- and 8-alkynyl-9-ethyladenines: synthesis and biological activity at human and rat adenosine receptors. *Purinergic Signal* 1:173–181
20. Richardson CM, Gillespie RJ, Williamson DS, Jordan AM, Fink A, Knight AR, Sellwood DM, Misra A (2006) Identification of non-furan containing A2A antagonists using database mining and molecular similarity approaches. *Bioorg Med Chem Lett* 16:5993–5997
21. Klotz KN, Kachler S, Lambertucci C, Vittori S, Volpini R, Cristalli G (2003) 9-Ethyladenine derivatives as adenosine receptor antagonists: 2- and 8-substitution results in distinct selectives. *Naunyn-Schmiedeberg's Arch Pharmacol* 367:629–634
22. CB BPG, Borea PA, Varani K, Pastorin G, Ros TD, Tabrizi MA, Fruttarolo F, Spalluto G (2002) Pyrazolo-triazolo-pyrimidine derivatives as adenosine receptor antagonists: a possible template for adenosine receptor subtype? *Curr Pharm Design* 8:2299–2332
23. Melman A, Wang B, Joshi BV, Gao ZG, Castro S, Heller CL, Kim SK, Jeong LS, Jacobson KA (2008) Selective A(3) adenosine receptor antagonists derived from nucleosides containing a bicyclo [3.1.0]hexane ring system. *Bioorg Med Chem* 16:8546–8556
24. Jaakola VP, Griffith MT, Hanson MA, Cherezov V, Chien EY, Lane JR, Ijzerman AP, Stevens RC (2008) The 2.6 angstrom crystal structure of a human A2A adenosine receptor bound to an antagonist. *Science* 322:1211–1217
25. Lakshmi PJ, Kumar BV, Nayana RS, Mohan MS, Bolligarla R, Das SK, Bhanu MU, Kondapi AK, Ravikumar M (2009) Design, synthesis, and discovery of novel non-peptide inhibitor of Caspase-3 using ligand based and structure based virtual screening approach. *Bioorg Med Chem* 17:6040–6047
26. Wei D, Jiang X, Zhou L, Chen J, Chen Z, He C, Yang K, Liu Y, Pei J, Lai L (2008) Discovery of multitarget inhibitors by combining molecular docking with common pharmacophore matching. *J Med Chem* 51:7882–7888
27. Mantri M, de Graaf O, van Veldhoven J, Goblyos A, von Frijtag Drabbe Kunzel JK, Mulder-Krieger T, Link R, de Vries H, Beukers MW, Brussee J, Ijzerman AP (2008) 2-Amino-6-furan-2-yl-4-substituted nicotinonitriles as A2A adenosine receptor antagonists. *J Med Chem* 51:4449–4455
28. Wei J, Wang S, Gao S, Dai X, Gao Q (2007) 3D-pharmacophore models for selective A2A and A2B adenosine receptor antagonists. *J Chem Inf Model* 47:613–625
29. Catalyst User Guide, Version 4.11 (Software Package) (2005) Accelrys Inc, San Diego, CA. <http://accelrys.com/>
30. Poptodorov K, Luu T, Hoffmann RD (2006) Pharmacophore model generation software tools. In: Langer T, Hoffmann RD (eds) *Pharmacophores and pharmacophores searches. Methods and principles in medicinal chemistry*. Wiley-VCH, Weinheim, pp 17–44
31. Güner OF (2000) Pharmacophore perception, development, and use in drug design. IUL Biotechnology Series. International UIniversity Line, La Jolla, CA. ISBN 0-96366817-6-1
32. Accelrys Software Inc (2004) *Discovery Studio Modeling Environment, Release 2.1*. Accelrys Inc, San Diego, CA. <http://accelrys.com/>
33. Kim J, Jiang Q, Glashofer M, Yehle S, Wess J, Jacobson KA (1996) Glutamate residues in the second extracellular loop of the human A2a adenosine receptor are required for ligand recognition. *Mol Pharmacol* 49:683–691
34. Toba S, Srinivasan J, Maynard AJ, Sutter J (2006) Using pharmacophore models to gain insight into structural binding and virtual screening: an application study with CDK2 and human DHFR. *J Chem Inf Model* 46:728–735
35. Kim HJ, Doddareddy MR, Choo H, Cho YS, No KT, Park WK, Pae AN (2008) New serotonin 5-HT(6) ligands from common feature pharmacophore hypotheses. *J Chem Inf Model* 48:197–206
36. Wang H, Duffy RA, Boykow GC, Chackalamannil S, Madison VS (2008) Identification of novel cannabinoid CB1 receptor antagonists by using virtual screening with a pharmacophore model. *J Med Chem* 51:2439–2446
37. Zampieri D, Mamolo MG, Laurini E, Florio C, Zanette C, Fermaglia M, Posocco P, Paneni MS, Priol S, Vio L (2009) Synthesis, biological evaluation, and three-dimensional in silico pharmacophore model for sigma(1) receptor ligands based on a series of substituted benzo[d]oxazol-2(3H)-one derivatives. *J Med Chem* 52:5380–5393